Supporting Information for On the Stability of Mantle-Sensitive P-waves Interference during a Secondary Microseismic Event

L. Tomasetto [1], P. Boué [1], L. Stehly[1], F. Ardhuin[2], H-C. Nataf [1]

[1]Univ. Grenoble Alpes, Univ. Savoie Mont Blanc, CNRS, IRD, Univ. Gustave Eiffel, ISTerre, 38000 Grenoble, France

[2]Laboratoire d'Océanographie Physique et Spatiale, University Brest, CNRS, IFREMER, IRD, Brest, France

This document details three aspects of the article. In particular, the geometries of networks used for subgroup selections, why we assumed uncorrelated noise sources in the formal modeling of cross-correlation functions, and the computation of travel times in 3D models using SeisTomoPy.

Contents of this file

1. Information on the Networks Used.
2. Uncorrelated Noise Sources
3. Travel Times in 3D Tomographic Models

Corresponding author: Lisa Tomasetto, Université Grenoble Alpes, ISTerre, CS 40700, 38058 GRENOBLE Cedex 9, FRANCE. (lisa.tomasetto@univ-grenoble-alpes.fr)

1. Information on the Networks Used

The networks selected for this study present high SNR and show diverse inter-station distances, numbers of cross-correlations, and paths, as seen in Figure 4c). The GR-KO network combination includes 174 station pairs between networks of the GR and KO. Both are permanent networks with a mean inter-station distance of around 25°. The second network combination contains 23 station pairs between the small array (KZ.KUR*) and a Malaysian seismic station, MY.KOM.00. Both are permanent networks with a mean inter-station distance of around 53°. The third network combination contains 54 station pairs between the network (ON) and the Transantarctic Mountains Northern Network (ZJ 2012-2015). ZJ(2012-2015) is a temporary experiment in Antarctica and ON a permanent network, the mean inter-station distance is around 84°.

2. Uncorrelated Sources

We here detail the simplification induced by the uncorrelated noise sources modeling. We use the formulation given in Chapter 4 of Nakata, Gualtieri, and Fichtner (2019) on modeling cross-correlations without retrieving the Green's Function. We start from the acoustic representation theorem which expresses recording at station A, $u_Z(x_A)$ depending on the Green's Function (G) computed in an Earth's velocity model (here PREM) and a forcing term (N) in the frequency domain:

$$u_Z(x_A) = \int G_{Z,Z}(x_A, \xi) N(\xi) d\xi \tag{1}$$

where the integral is conducted over all potential source locations ξ, the dependence in frequency is not explicit here. So the cross-correlation between vertical components of

station A and station B can be expressed as:

$$C_{ZZ}(x_A, x_B) = u_Z(x_A)u_Z^*(x_B) = \int_{\partial D}\int_{\partial D} G_{ZZ}(x_A, \xi_1)G_{ZZ}^*(x_B, \xi_2)N(\xi_1)N^*(\xi_2)d\xi_1 d\xi_2 (2)$$

where * denotes the complex conjugate and ∂D is the domain of potential sources (the ocean surface here). The spatially uncorrelated noise sources assumption allows us to reduce the right term to a simple integral. Let us take two potential source locations $(x, y) \in \partial D^2$, the sources are considered spatially uncorrelated if $\langle N(x)N^*(y)\rangle = S(x)\delta(x-y)$ simplifying the cross-correlation expression as given in section 4.2. The expression retrieved simplifies the model of cross-correlation functions with a low computation cost. Oceanic sources of seismic waves can be spatially correlated when considering waves breaking on coastal areas, as described in Ayala-Garcia, Curtis, and Branicki (2021). In the case of a secondary microseism source, one cannot ensure that sources are uncorrelated. Since correlated sources generate repeating patterns and spurious arrivals in the cross-correlation Ayala-Garcia et al. (2021) that are not seen in our data, we assume that the sources are uncorrelated. Also, the grid of sources we use has a 55 km width in latitude and longitude, we assume that the sources have uncorrelated behavior due to the different bathymetry and sea state. In summary, we assume the sources are spatially uncorrelated by default in the absence of evidence of correlated sources. However, the impact of correlated sources on our synthetic modeling of correlations needs to be further studied.

3. Travel Times in 3D Tomographic Models

To compare our travel times measurements between synthetic and data-based cross-correlations with expected values, we computed the ray theory equivalent using the SeisTomoPy package (Durand et al., 2018). V_P is scaled from V_S, using the Poisson ratio ν_α

such that $d\ln(V_P) = \nu_\alpha d\ln(V_S)$, the value of ν_α given for models SEISGLOB2, S40RTS, S362WMANI+M, SEMUCB-WM1 and SGLOBE in Table S2. For each subgroup, the barycenter of each network was used as station A and station B locations, and the reference storm location as the source location. The sections of ray paths used are represented by Figure S1. As explained in the main text, we compute delays to the $PP-P$ interference travel time in PREM for a list of available 3D models as follows:

$$dt_{3Dth} = t^{PP}_{3D}(SB) - t^{P}_{3D}(SA) - (t^{PP}_{1D}(SB) - t^{P}_{1D}(SA)) \tag{3}$$

with 3D varying in SEISGLOB2, S40RTS, S362WMANI+M, SEMUCB-WM1, SGLOBE, MITP08, DETOX-P3 and SP12RTS. All computed travel times are summed up in Table S1. The 1D model travel times in PREM are corrected by the ellipticity of the Earth's using the EllipticiPy package (Russell et al., 2022) so that :

$$t^{P}_{1D}(SB) = t^{P}_{PREM}(SB) + dtell^{P}_{PREM}(SB) \tag{4}$$

where $dtell^{P}_{PREM}(SB)$ is the ellipticity correction for a P wave travel time in PREM between the source and barycenter B positions.

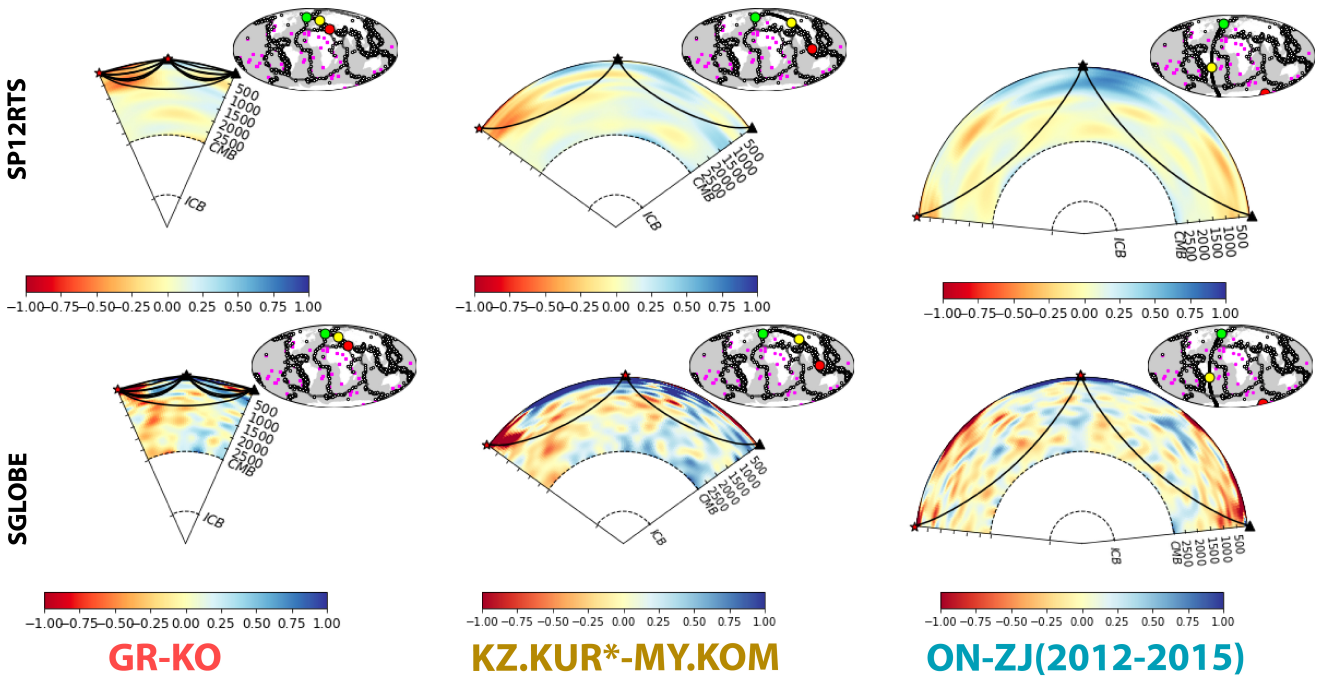

Figure S1. SeisTomoPy ray paths output for the three subgroups in the SP12RTS and SGLOBE models. From left to right: GR-KO, KZ.KUR*-MY.KOM, ON-ZJ(2012-2015). The maximum velocity perturbation for the color bar is 1%.

Model	GR-KO	KZ.KUR*-MY.KOM	ON-ZJ
SEISGLOB2	0.34s	-1.86s	-7.08s
S40RTS	-0.35s	-2.04s	-6.45s
S362WMANI+M	5.88s	-2.36s	-7.05s
SEMUCB-WM1	-3.2s	-2.23s	-6.71s
SGLOBE-rani	-0.97s	-2.52s	-6.21s
SP12RTS	-0.43s	-1.89s	-6.75s
MITP08	-0,34	-3,15	-7,34
DETOX-P3	0,13	-1,95	-5,78
Mean	0,13	-2,25	-6,67

Table S1. Table of Travel Times for PP-P interference measured for different 3D models using SeisTomoPy.

S-wave Model	ν_α
SEISGLOB2	0.55
S40RTS	varies from 2 (surf) to 3 (CMB)
S362WMANI+M	0.55
SEMUCB-WM1	0.5
SGLOBE-rani	0.5

Table S2. Scaling factor values taken from SeisTomoPy documentation.

References From the Supporting Information

Ayala-Garcia, D., Curtis, A., & Branicki, M. (2021). Seismic interferometry from correlated noise sources. *Remote Sensing*, *13*(14), 2703.

Durand, S., Abreu, R., & Thomas, C. (2018). Seistomopy: fast visualization, comparison, and calculations in global tomographic models. *Seismological Research Letters*, *89*(2A), 658–667.

Nakata, N., Gualtieri, L., & Fichtner, A. (2019). *Seismic ambient noise*. Cambridge University Press.

Russell, S., Rudge, J. F., Irving, J. C., & Cottaar, S. (2022). A re-examination of ellipticity corrections for seismic phases. *Geophysical Journal International*, *231*(3), 2095–2101.